



CMD 23-M36.5

Date: 2023-10-30

File / dossier : 6.02.04

Edocs pdf : 7157801

## **Oral presentation**

## **Exposé oral**

**Written submission from  
Paul Sedran, RESD Inc.**

**Mémoire de  
Paul Sedran, RESD Inc.**

---

Regulatory Oversight Report for  
Canadian Nuclear Power Generating  
Sites: 2022 and Mid-term update for  
Ontario Power Generation's Pickering  
Nuclear Generating Station

---

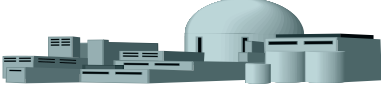
Rapport de surveillance réglementaire  
des sites de centrales nucléaires au  
Canada : 2022 et Rapport de mi-parcours  
d'Ontario Power Generation pour la  
centrale nucléaire de Pickering

Commission Meeting

Réunion de la Commission

**December 13 and 14, 2023**

**13 et 14 décembre 2023**

 <b>RESD Inc.</b>	<b>Document Identification</b>				
	<small>Project</small>	<small>Type</small>	<small>Division</small>	<small>Serial</small>	<small>Revision</small>
	<b>CNSC 005</b>	<b>REPT</b>	<b>ENG</b>	<b>0001</b>	<b>00</b>
<small>Date Effective:</small>			<small>Retain Until:</small>		
<b>Oct 30, 2023</b>			<b>Oct 30, 2030</b>		

Review of Submissions for the Midterm Review of  
Licensed Activities for Pickering NGS



Prepared by: Paul Sedran, P.Eng  
Principal, RESD Inc

Date: October 30th, 2023

## Definition of Abbreviations and Symbols

CT	Calandria Tube
CTS	Calandria Tube Sheet
DHCV	Delayed Hydride Cracking Velocity
LSFCR	Large Scale Fuel Channel Replacement
NGS	Nuclear Generating Station
PLGS	Point Lepreau Generating Station
PNGS	Pickering Nuclear Generating Station
PT	Pressure Tube
S1	Spacer 1
S2	Spacer 2
S3	Spacer 3
S4	Spacer 4
x	Axial Position along the length of the Fuel Channel
y	Vertical Deflection

# 1. Introduction

OPG currently holds a ten year operating license for the Pickering Nuclear Generating Station (PNGS) which is valid for the period from September 1st, 2018, to August 31st, 2028. At the time of the license application, OPG intended to cease commercial operation of PNGS on December 31, 2024, such that licence period would cover three phases of operational activities: continued commercial operation until December 31, 2024; a stabilization phase (post-shutdown defuelling and dewatering) of two to three years; and the beginning of safe storage for six reactor units, which would mark the beginning of station decommissioning.

September, 2023 will mark the midpoint for the current ten year operating license. The CNSC will be conducting a public hearing for the Midterm Review of OPG's license-related activities for PNGS, scheduled for December, 2023. The Midterm Review covers activities within the period from September 1st, 2018, to September 2023. OPG's main written submission for the public hearing, Reference [1], identified in Section 2.1, provides updates for the PNGS Midterm Review. In addition to the Midterm Review for PNGS, the public hearing will cover a review of the CNSC's regulatory oversight report for 2022, referenced in Section 2.1.

The CNSC, under Contribution Agreement reference number: PFP 2023 PNGS ROR CA has funded the author to review submissions to the public hearing, which are specified in Section 2.1 (including related documents referred to in Section 2.2) from the perspective of Fuel Channel fitness-for-service, and to comment on integrity issues for the PNGS Fuel Channels.

The review of the submissions identified in Section 2.1, from the perspective of Fuel Channel fitness-for-service, has been completed. Comments, observations, and suggestions from the review of Reference [1] have been documented in Section 3 of this report. Comments from the review of Reference [2] are found in Section 4.

As part of the review of Fuel Channel fitness-for-service for PNGS, the author has taken the opportunity provided by this intervention to present OPG with comments on a long-standing industry practice related to the calibration of CT-PT gap measurements, which forms the main part of this report. Although gap calibration was initiated much earlier than the time period for the Midterm Review, the author believes that OPG has continued to use gap calibration throughout the Midterm Review period, so that gap calibration is an appropriate topic for this review.

## 2. Reference Documents

### 2.1 Submissions Released to the Intervenors by the CNSC

The following public hearing documents were released to the intervenors prior to the public meeting and were reviewed by the author:

1. Mid-Term Update of Licensed Activities for the Pickering Nuclear Generating Station, CMD 23 M36.1 [1].
2. Regulatory Oversight Report for Canadian Nuclear Power Generating Sites for 2022, CMD 23-M36 [2].

## 2.2 PNGS Fuel Channel Documents Related to Reference [1]

In Reference [1], the Fuel Channel Life Cycle Management Plans, (LCMP)s were mentioned directly and fitness-for-service assessments were discussed. Therefore, the conclusions of Reference [1] are based on the LCMP and the corresponding fitness-for-service assessment documents. The dependence of Reference [1] on the Fuel Channel LCMPs and the fitness-for-service assessments would bring the LCMP and fitness-for-service assessment documents prepared over the review period into the scope of the PNGS Midterm review.

However, for this review, these documents were not requested from OPG because of time constraints. Instead, the author chose to focus the review of PNGS Fuel Channel fitness-for-service issues on the select technical issue of CT-PT gap calibration, as mentioned in the introduction. Gap calibration is related to Fuel Channel fitness-for-service assessment and is considered to be within the scope of the Midterm Review for PNGS.

## 3. Review of Reference [1]

The following article on Page 41 of Reference [1] was reviewed.

### ***Fuel Channels***

*The Canadian Standards Association (CSA) Standard N285.4 prescribes requirements for monitoring fuel channel conditions via periodic inspections of multiple fuel channels. This standard also prescribes material surveillance which requires harvesting both small (thin scrape) and large (removal of entire pressure tube (PT)) samples of PT material for subsequent destructive testing at a specialized laboratory facility to confirm material properties. The CSA Standard N285.4 standard defines acceptance criteria that must be met for given fuel channel conditions. If a fuel channel condition satisfies these acceptance criteria, then that condition is considered unconditionally acceptable, as the fuel channel remains within the design basis. OPG will continue to address the issues related to component aging with high regard for nuclear safety and transparency with CNSC staff. OPG is committed to ongoing active participation in research and development (R&D) programs designed to improve the understanding of aging mechanisms and improvement of assessment tools and methodologies for the assessment of fitness-for-service. Based on inspections, assessments, R&D work completed to date, confirmatory actions in the LCMPs for assuring ongoing fitness-for-service, and use of mitigating actions where required, OPG is confident of continued safe operation of Pickering NGS Major Components to the assumed service life targets. The fuel channel program produces fitness-for-service assessments that are aligned with all licensing requirements. Based on the established programmatic controls for managing fuel channel aging, which include an extensive reactor inspection program, sound technical assessments, and the implementation of mitigating measures where required.*

Comments resulting from the review are provided in Section 3.1.

As part of the review, the author has produced an example of a recommended text for the article in question, which is presented in Section 3.2.

Section 3.3 covers a select review of the technical issue of gap calibration, related to Reference [1], since it has an influence on Fuel Channel fitness-for-service assessments for PNGS.

### **3.1 Comments on the text on Fuel Channels in Reference [1]**

In general, Reference [1] provides current information to update the reader on a multitude of specific topics related to the licensing of PNGS. In Reference [1], OPG has the latitude of providing updates to cover the most recent events only or providing a more comprehensive update that elaborates on all significant events over the last five years.

For The text covering Fuel Channel fitness for service, it is proposed that some historical information is provided to update the reader on all events over the time period for Midterm Review.

The text covering Fuel Channel fitness for service correctly identifies CSA N285.4 as the document that specifies Fuel Channel inspection requirements. In the description of CSA N285.4, some information on material surveillance is provided, but there is no equivalent information on periodic inspections such as ultrasonic flaw detections, PT gauging measurements, and PT-CT gap measurements. Therefore, there is more focus on material surveillance than on the other types of inspections required by CSA N285.4, which is not an accurate reflection of CSA N285.4 and might be misleading for some of the readers.

In the discussion of large and small samples for material surveillance, there is mention of thin scrape samples, but no mention of PT cut end samples that are shipped with the end fitting for testing with the end fitting. Also, there is no elaboration in the text on the material testing specimens that are machined from the removed PT, such as small specimens for DHCV and fracture toughness testing.

As written in the text, CSA N285.4 does mention acceptance criteria for some Fuel Channel conditions. However, the text neglects to state that the numerical values of the acceptance criteria are given in Annex D of CSA N285.8

### **3.2 Suggested Wording for the Text on Fuel Channels in Reference [1]**

Although the existing wording is generally adequate for the purposes of the Midterm Update by OPG, the author has identified some changes to improve the technical accuracy of the text.

Those changes have been incorporated into the text that follows:

*The Canadian Standards Association (CSA) Standard N285.4 prescribes requirements for monitoring fuel channel conditions via periodic inspections of multiple fuel channels at defined periods of time in-service.*

*The standard prescribes (1) non-destructive inspections such as ultrasonic pressure tube (PT) flaw detection, ultrasonic PT gauging measurements, and electrical capacitance measurements of Calandria Tube (CT) to PT gap and the eddy current detection of axial spacer locations and (2) destructive material surveillance testing, which requires harvesting*

*both small (thin scrape) samples and large samples of PT material ( the entire PT and PT cut ends) for subsequent destructive testing at a specialized laboratory. The thin scrape samples are used for chemical analysis to measure hydrogen and deuterium concentrations, while the large samples are used to machine material test specimen for fracture toughness and delayed hydride crack velocity testing.*

*The CSA Standard N285.8 standard defines acceptance criteria that must be met for given fuel channel conditions. If a fuel channel condition satisfies these acceptance criteria, then that condition is considered unconditionally acceptable, as the fuel channel remains within the design basis. OPG will continue to address the issues related to component aging with high regard for nuclear safety and transparency with CNSC staff. OPG is committed to ongoing active participation in research and development (R&D) programs designed to improve the understanding of aging mechanisms and improvement of assessment tools and methodologies for the assessment of fitness-for-service.*

*Based on inspections, assessments, R&D work completed to date, confirmatory actions in the LCMPs for assuring ongoing fitness-for-service, and use of mitigating actions where required, OPG is confident of continued safe operation of Pickering NGS Major Components to the assumed service life targets. The fuel channel program produces fitness-for-service assessments that are aligned with all licensing requirements. Based on the established programmatic controls for managing fuel channel aging, which include an extensive reactor inspection program, sound technical assessments that use the acceptance criteria of the nation standard, CSA N285.8 and the implementation of mitigating measures where required.*

### **3.3 Review of Gap Calibration for the PNGS Fuel Channels**

One technical finding related to PNGS Fuel Channel integrity arose from the Midterm Review. The finding pertains to the particular method used to generate CT-PT calibrated gap values that are used as inputs into probabilistic time-to-contact computations.

The background for gap calibration and the related finding is explained and discussed in the sections that follow.

Section 3.3.1 defines how CT-PT gap values are used in probabilistic CT-PT time-to-contact predictions. A description of the calibration of CT-PT axial gap profiles to produce CT-PT gap values for use in probabilistic CT-PT time-to-contact predictions is presented in Section 3.3.2.

Section 3.3.3 presents a technical issue with the gap calibration that was discovered by the author several years ago, which represents the main point of this report and the intervention.

#### **3.3.1 The use of CT-PT Gap Values in probabilistic CT-PT time-to-contact predictions.**

In the probabilistic analysis of CT-PT contact, each Fuel Channel simulation involves the computation of the creep sag of the PT and the CT over time in-service. PT end slope and the creep factor are significant input parameters in the engineering model used to compute Fuel Channel creep sag in each simulation.

The method for determining the input values of PT end slope and creep factor for a given Fuel Channel with CT-PT gap measurements, for creep sag simulation, involves:

1. Extracting axial profiles of measured CT-PT gap at the bottom of the Fuel Channel from the in-service inspection data,
2. Calibrating the individual gap measurement data points in the axial gap profile, as defined below,
3. Performing multiple iterations of the following computation steps: :
  - a. Executing the Fuel Channel creep sag model to compute predicted CT-PT gap values with trial PT end slope and creep factor values,
  - b. Comparing the predicted CT-PT gaps from Step 2, to the calibrated gap measurement data points for the same Fuel Channel,
  - c. Adjusting the PT end slope and creep factor input values and repeating the Fuel Channel creep sag computation with the adjusted input values.

The iterative computations in Steps 3a, 3b, and 3c are repeated until the computed CT-PT gap values match the calibrated gap measurement data points, which constitutes the converged iteration.

The PT end slope and creep factor input values for the converged iteration were taken as the official input values for further probabilistic analysis of the given Fuel Channel.

### 3.3.2 Details of the Gap Calibration Method

Regarding Step 2 above, the calibration of the gap measurement data is performed on the basis that the actual magnitude of the in-service gap at spacer locations is determined entirely by the design basis dimension of the outer diameter of the spacer coil, (5.59 mm for the CANDU 6 reactor).

In practical terms, the calibration is performed by (1) increasing the measured gap values at the spacer locations to match the design basis outer diameter of the spacer coil, and (2) adjusting the gaps at various other points along the axial gap measurement profile accordingly.

An example of gap calibration is presented in Figure 1, which presents gap measurements and calibrated gap measurements from the 2005 inspection of Fuel Channel H14 in Gentilly-2, referred to as G2H14. The figure was reproduced from Reference [3]. In the figure, the magnitude of the measured gap at the bottom of the CT is plotted on the Y axis and the axial location (with respect to the Calandria Tube Sheet (CTS) ) at which the gap was measured, is plotted on the X axis. The points along the Y axis coincide with the outer diameter at the bottom of the PT, such that the sum of the PT outer radius plus the gap would equal the CT inner radius, at a given axial location.

The blue line in Figure 1 represents the actual gap measurements recorded in the inspection. The red line in Figure 1 represents the calibrated gap measurements for Fuel Channel G2H14.

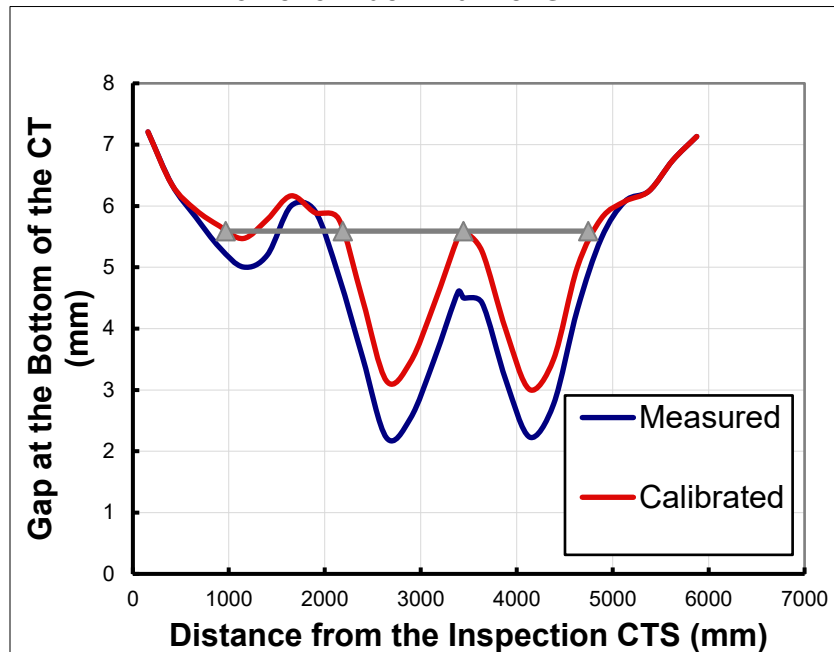
The four grey triangles located on the horizontal grey line in Figure 1 represent the gap at the bottom of the Fuel Channel that would result from four spacers with a spacer coil design outer diameter of 5.59 mm separating the bottom of the PT and the CT. The axial positions of the grey triangular points in Figure 1 are located at the detected locations of the four spacers in Fuel Channel H14. The y coordinate of the four points is at  $y = 5.59$  mm, which represents the design basis outer diameter of the spacer coil.



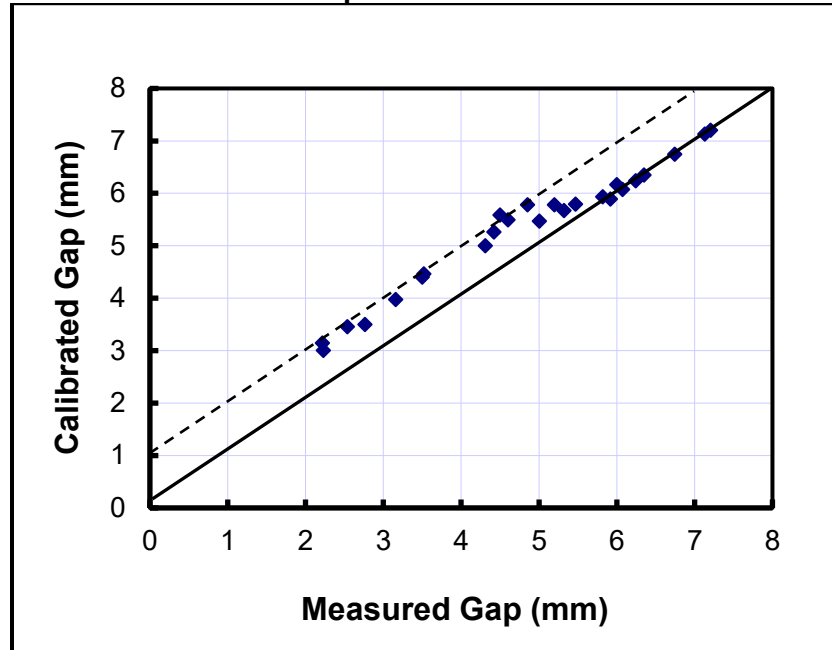
The gap calibration is depicted in Figure 1 as the adjustment of the measured gap profile to produce the calibrated gap profile, achieved by moving the measured gap profile such that the resultant gap at the four spacer locations equals the spacer coil outer diameter, 5.59 mm

Figure 2 presents a plot of the calibrated gap values versus the measured gap values for the gap profiles shown in Figure 1. As seen in Figure 2, the measured gaps of 6 mm or greater were not calibrated. The gaps of 5.5 mm or less were calibrated and most of the calibrated gaps were generated by adding less than 1 mm to the corresponding gap measurement.

**Figure 1**  
**Example of the Calibration of the Axial Gap**  
**Profile for Fuel Channel G2 H114**



**Figure 2**  
**Plot of Calibrated Gap versus**  
**Measured Gap for Fuel Channel G2H14**



It is apparent from Figure 1 and 2 that gap calibration results in an increase in the magnitude of the gap for each point along the axial gap profile, except for the points at the beginning and end of the axial gap profile, where gap calibration has no effect on the gap. As an example, for the gap at 2640 mm from the CTS, calibration will raise the gap from 2.22 to 3.10 mm, for an increase of 0.88 mm. In most structural components, a deformation of less than 1 mm would have negligible mechanical consequences.

However, in this case, a 0.88 increase in gap at the 2640 mm axial location represents an increase of 39.6%, compared to the actual gap measurement at 2640 mm. For the Fuel Channel with the axial gap profiles depicted in Figure 1, an increase of 0.88 mm in the gap at 2460 mm will result in a significant increase in the predicted onset time for CT-PT contact.

Therefore, the gap calibration method depicted in Figure 1 has the following implication for CT-PT time-to-contact predictions. Since predicted CT-PT time-to-contact values, based on calibrated gaps, are greater than the corresponding time-to-contact predictions with no gap calibration, then gap calibration would result in overestimations of time-to-contact, compared to time-to-contact predictions with no gap calibration.

As a result, the gap calibration method in question could potentially have a negative effect on the level of conservatism present in CT-PT time-to-contact predictions and so it merits a considerable amount of scrutiny and technical justification.

### **3.3.3 Technical Implication of the Gap Calibration Method – Implied CT Dimensions**

In 2005, the author was involved in the analysis of CT-PT gap measurements from in-service inspections of various Fuel Channels in PLGS. From an investigation of PT in-service

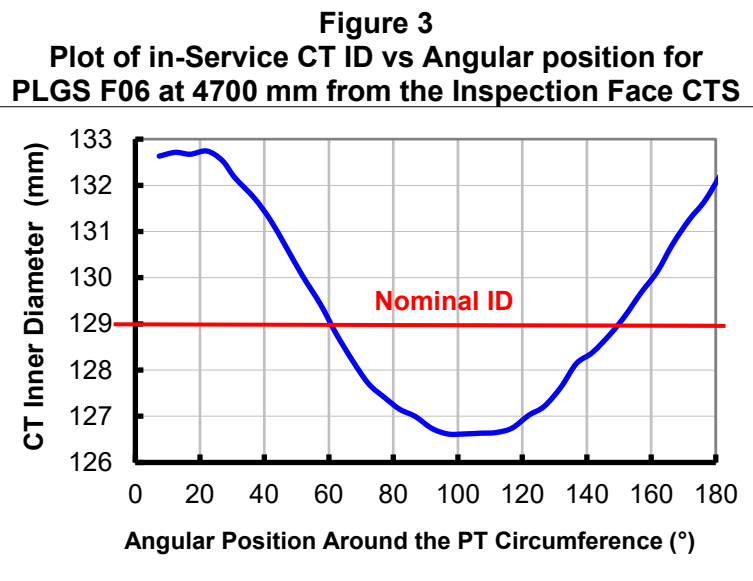
ultrasonic gauging results and CT-PT gap measurements, it was determined that PT Inner Diameter (ID), PT wall thickness, and PT-CT gap measurements, all at a given location for a given time in-service, could be combined to calculate in-service CT ID values. It should be noted that when the CT-PT gap measurement probes were under development, CT-PT gap measurement was the primary objective, with no consideration for the possibility of using the gap measurements to determine CT ID.

Details of the method for calculating in-service CT IDs using PT gauging and CT-PT gap measurements from in-service inspections are provided in Reference [3].

The method is very simple and is based on the fact that the CT inner radius at any axial position along the length of the CT, and at any angular position around the circumference of the CT, is the sum of the corresponding PT inner radius, plus the corresponding PT wall thickness and the CT-PT gap measurement.

The calculation method outlined in Reference [3] was used to generate in-service axial and circumferential CT ID profiles for various Fuel Channels in PLGS, in Gentilly-2, and in Bruce B.

As an example, a typical in-service CT ID circumferential profile at a spacer location is presented in Figure 3. Figure 3, as discussed in detail in Reference [3], indicates the development of ovality in the shape of the CT cross-section at the spacer location as a result of the vertical spacer load on the PT.



Having generated in-service CT ID values for a number of Fuel Channels, the next logical step consisted of investigating the validity of the CT ID values.

It was subsequently realised that in-service CT ID values could be generated using either actual gap measurements or calibrated gap measurements and that a comparison of the ensuing CT ID values would yield some useful results. Following this train of thought, a comparison of in-service CT IDs generated with and without gap calibration was carried out for the purpose of investigating the validity of the gap calibration method in question.

For this purpose, the axial CT ID profiles presented in Figures 4 and 5 were prepared.

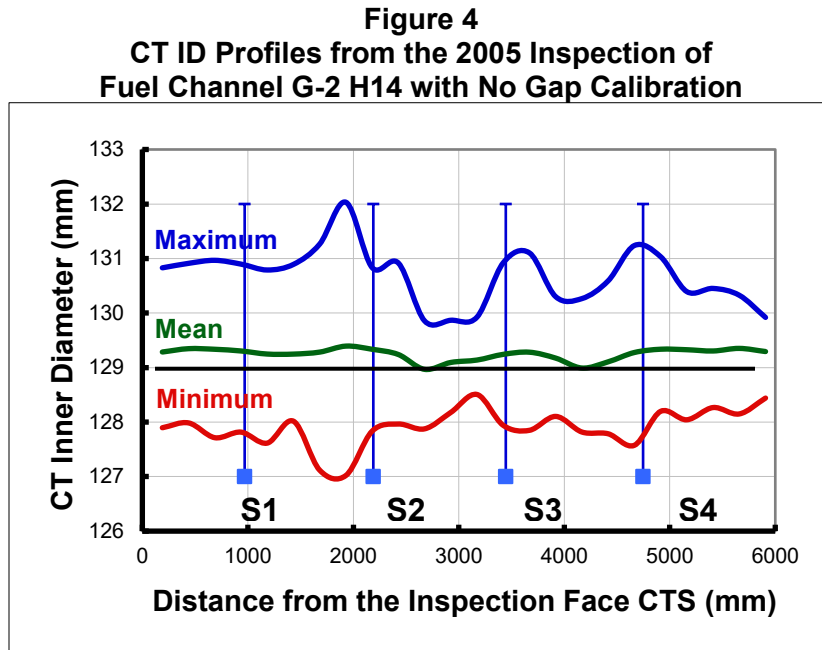
In the two figures, three separate CT ID profiles have been plotted. The lower lines in the graphs, plotted in red in Figures 4 and 5, represent the minimum CT ID at a given axial location versus axial position along the length of the CT. The green lines in the middle of the graphs in Figures 4 and 5 represent the mean CT ID at a given axial location versus axial position along the length of the CT. Lastly, the blue lines at the top of the graph in Figures 4 and 5 represent the maximum CT ID at a given axial location versus axial position along the length of the CT.

The CT ID profiles in Figure 4 are from the 2005 inspection of Gentilly-2 (G-2) and the profiles of Figure 5 are from the 2004 inspection of Point Lepreau (PLGS)

Note that spacer locations are indicated with vertical lines in Figures 4 and 5 and that the labels S1 –S4 on the spacer locations stand for Spacer 1 – Spacer 4.

Some details of the generation of the profiles presented in Figures 4 and 5 are provided in Reference [3] and are discussed later in the report.

The critical point in comparing Figures 4 and 5 is that actual gap measurements were used in the generation of the CT ID profiles in Figure 4, whereas in Figure 5, calibrated gap measurements were used.

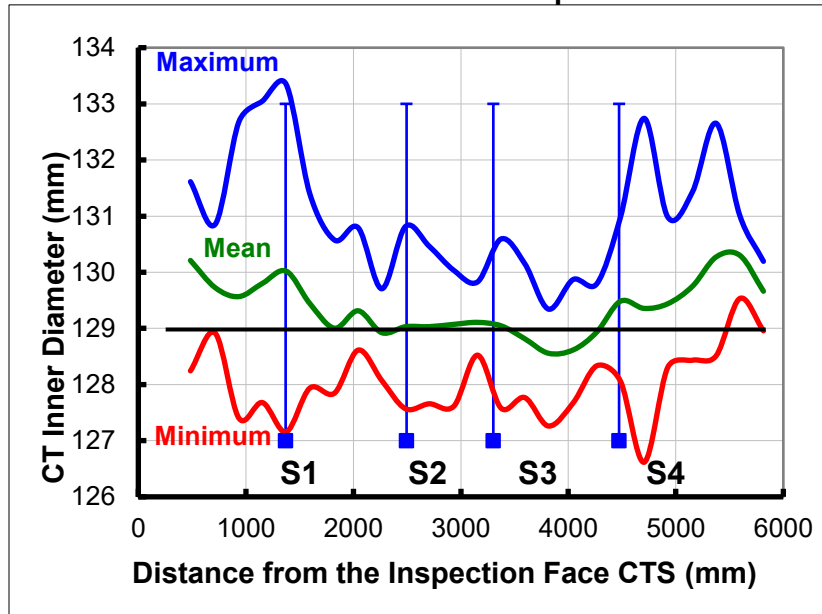


The thick horizontal black line in Figures 4 and 5 represents the nominal as-installed diameter of the CT, 129.0 mm.

Examining Figure 4, it is seen that, with no gap calibration, the CT mean ID is somewhat uniform, with a range of 0.393 mm, over the length of the CT in G-2 H14.

In contrast, as shown in Figure 5, with gap calibration, the mean CT ID is almost uniform only between Spacers 2 and 3 but varies significantly of the length of the CT in PLGS F06. With gap calibration, 1.74 mm is the range in the mean CT ID.

**Figure 5**  
**CT ID Profiles from the 2004 Inspection of**  
**Fuel Channel PLGS F06 with Gap Calibration**



The above comparison of Figure 4 with Figure 5 establishes that there is an actual difference in the mean CT ID profiles generated with and without gap calibration, which is expected, since the CT ID partially depends on the gap.

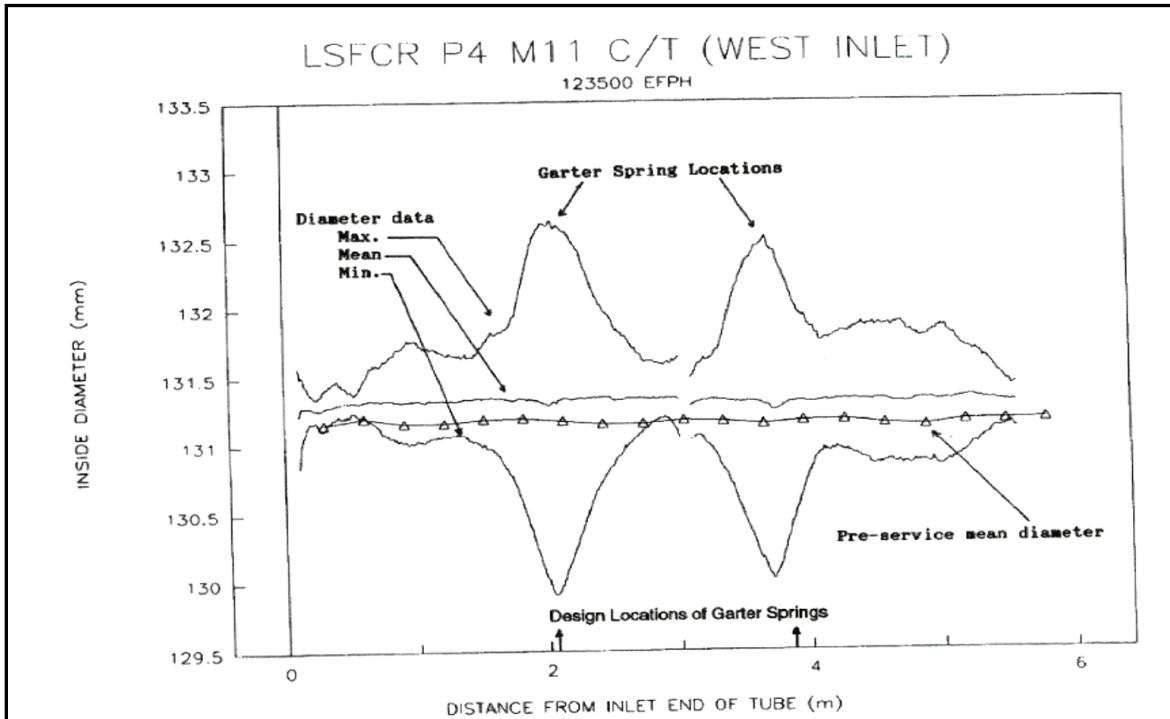
Having established that there is an influence of gap calibration on CT ID profiles, the next step in the investigation was to explore the validity of the CT ID profiles generated with gap calibration versus those generated without.

For this purpose, a survey of gauging measurements from CTs that had been removed from reactors was conducted. At the time of the survey, about ten different ex-service CTs from different reactors had been examined and were subject to gauging measurements, which were used to produce CT ID profiles, of the same type as Figures 4 and 5.

The gauging measurements from one particular ex-service CT were selected for further study. The selected gauging measurements were for the CT that was removed from Fuel Channel M11 in Pickering Unit 4 (P4) at the time of the P4 LSF CR.

Figure 6, reproduced below from Reference [3], presents maximum, mean, and minimum CT ID measurements versus axial position along the length of the CT from P4 M11.

**Figure 6**  
**ID Profiles from the Ex-Service Gauging of the CT**  
**Removed from Fuel Channel M11 for LSF CR**



Figures 4, 5, and 6 all display the common feature of having peak maximum CT inner values and peak minimum CT ID values at or near spacer locations. As outlined in Reference [3], the local peak in the maximum ID of the CT at the spacer location is readily explicable from the effect of spacer loading of the CT. The same applies to the local peak (actually, a local minima) in the minimum ID of the CT at the spacer location.

Essentially, the cross-sections of the CT at the spacer locations have been deformed into an ovalised shape as a result of vertical in-service spacer loading, which is consistent with CT ID profile seen in Figure 3.

It is also observed in Figure 6 that the mean in-service CT ID is practically uniform over the length of the CT and closely matches the as-installed CT ID value at each point along the length of the CT to within 0.2 mm, noting that the in-service mean ID of the CT is slightly greater than the mean as-installed ID.

The geometry of the spacer and CT is such that the initial area of contact is confined to a point at the bottom of the CT. With in-service creep of the CT, the contact point will develop into an area of contact, consisting of a short, narrow arc, at the bottom of the CT. The load of the spacer on the bottom of the CT will generate bending at the bottom of the CT and tensile hoop stresses on the sides of the CT. Considering that the spacer load would consequently be applied in a short, narrow area at the bottom of the CT, circumferential bending of the CT is expected to be the dominant mode of deformation of the cross-section of the CT that was under spacer loading.

Consequently, under in-service spacer loading, circumferential bending would result in an increase in the vertical ID and a decrease in the horizontal ID but with no increase in the circumference of the CT.

Similarly, it is expected that the tensile hoop stresses at the side of the CT would result in a small amount of circumferential strain.

Looking at Figure 6, it is evident that CT M11 from Pickering Unit 4 displays circumferential bending deformation, leading to ovality at the spacers plus a small amount of circumferential expansion.

Comparing Figures 4 and 5 with Figure 6, it is seen that the mean in-service CT ID profile for P4M11 (Figure 6) is more consistent with the profile of Figure 4 than with the profile of Figure 5.

On the basis of the similarity between Figures 4 and 6 and the discussion of spacer loading, above, the conclusion is that the actual in-service deformation of the CT should feature a near-uniform mean ID profile, with a slight diametral expansion relative to the as-installed mean diameter of the CT, which was evident in P4 M11, in Figure 6.

However, with gap calibration, using PLGS F06 as an example, the mean ID of the CT is non-uniform over the length of the CT and features significant diametral expansion, not seen in P4 M11.

Therefore, it is proposed that the gap calibration scheme used to produce the CT ID profiles for PLGS F06 of Figure 5, assuming that no other unexplored factors are at play, resulted in an overestimation of various gap values, manifested in Figure 5 as an overestimation of the CT mean ID at different points along the CT.

If the above proposition is correct, the implication is that the gap calibration scheme in question is technically incorrect, since the calibrated gaps, when used to generate in-service CT ID profiles, result in unrealistic CT ID values, i.e. profiles that do not match those for P4 M11.

Therefore, in order for the Fuel Channel analysts to continue to use the gap calibration scheme for the PNGS Fuel Channels, there should be an investigation into the effect of the calibrated gaps on the resultant CT ID profiles. The investigation would be to determine if the irregular CT mean ID profiles of Figure 5 are attributable to gap calibration alone.

If so, then the recommendation would be that OPG discontinue the use of gap calibration in the interpretation of gap measurement results for the PNGS Fuel Channels. One possibility is that the measured gap values (without calibration) could be used in Fuel Channel fitness-for-service assessments for PNGS, instead of the calibrated gap values.

### **3.3.4 The Effect of Gap Calibration on Predicted PT-CT Contact Times**

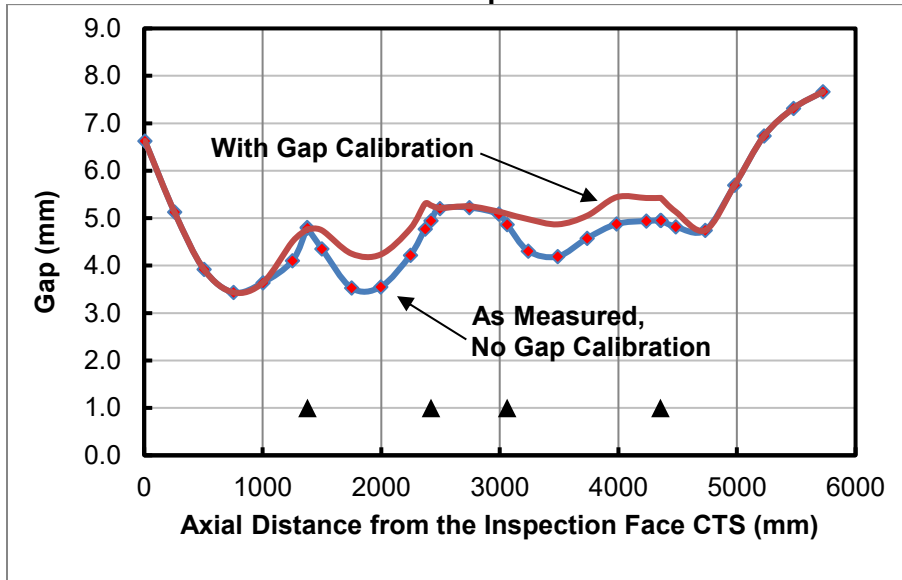
This section presents an example of comparative CT-PT time-to-contact predictions, with and without gap calibration, to demonstrate the effect of gap calibration on calculated contact times.

Originally, it was intended that the comparative time-to-contact analysis would be performed for a specific Fuel Channel in PNGS, but the information transfer process from OPG, to obtain

PNGS-specific technical data, turned out to be impractical for this particular intervention. Instead, the comparative analysis was performed for G2K07, which was inspected in 2005, at 161,000 EFPH on the basis that G2K07 would be similar to a number of the Fuel Channels in PNGS. Although the G2 Fuel Channels are slightly different to those in PNGS, the effect of gap calibration in the comparative analysis of G2K07 is expected to be representative of that in the PNGS Fuel Channels

Figure 7 presents as-measured and calibrated gap profiles for G2K07. It should be noted that in the gap calibration scheme for G2K07, the calibrated gaps at the spacer locations, shown as the black triangles in Figure 7, do not exactly match 5.59 mm. An important point regarding Figure 7 is that the measured CT-PT gaps are with the Fuel Channel in inspection configuration, under reduced loading compared to in-service loading, described later. Actual in-service gaps will be slightly smaller than those in Figure 7 and can be calculated from the measured gaps.

**Figure 7**  
**As Measured and Calibrated Gaps for G2K07 versus**  
**Distance from the Inspection Face CTS**



Note that the points on the gap profiles of Figure 7 and Figures 8 and 9, presented later, coincide with points that are approximately at the bottom of the PT and represent the approximate shape of the PT.

The measured spacer locations for G2K07 are presented in Table 1.



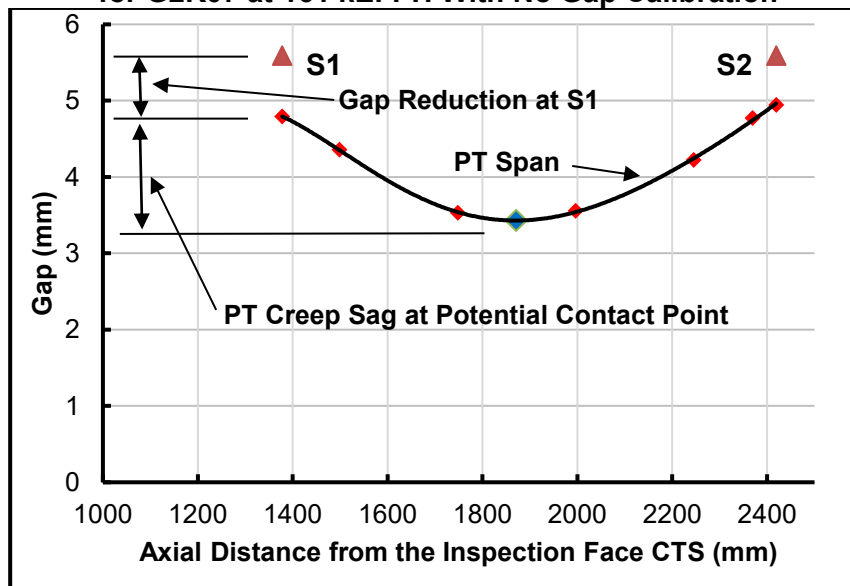
**Table 1**  
**Spacer Locations relative to the Inspection Face CTS**

Spacer	x (mm)
S1	1378
S2	2419
S3	3061
S4	4353

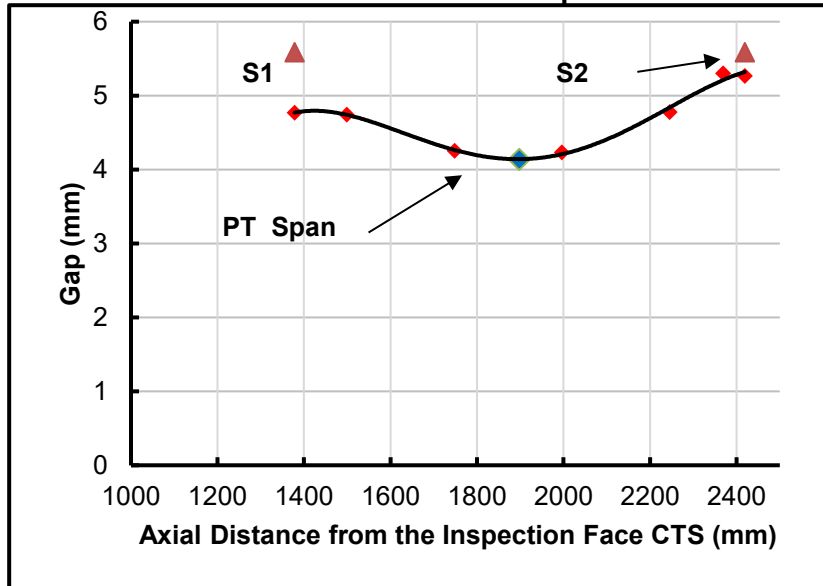
For the time-to-contact analysis, contact of the second span of the PT with the CT was considered. The second span of the PT is that which is supported by S1 on the left end and supported by S2 on the right end, as depicted in Figure 7. The x coordinate of the contact point for the second span was determined by interpolation of the PT sag profile to be  $x = 1870.4$  mm. Similarly, the as measured gap at 1870.4 mm was determined to be 3.430 mm.

Figure 8 shows the configuration of the as-measured gap profile between S1 and S2. The corresponding calibrated gap profile is shown in Figure 9. The blue points on the as-measured and calibrated gap profiles represent the axial location of the local minimum gap between the CT and the PT at the time of the inspection. For the as-measured gap profile  $x = 1870.4$  mm, and for the calibrated gap profile,  $x = 1897.9$  mm which are axial positions of the potential contact points of the PT with the CT, for the two gap profiles.

**Figure 8**  
**Illustration of the PT Span Between S1 and S2**  
**for G2K07 at 161 kEFPH With No Gap Calibration**



**Figure 9**  
**Illustration of the PT span between S1 and S2**  
**for G2K07 at 161 kEFPH With Gap Calibration**



The two red triangles near the top of Figures 8 and 9 represent the 5.59 mm gap that would be provided by the spacers at the time of installation.

In Figure 8, it is seen that the gap at the potential contact point is determined by the gap reduction at the spacer locations and the lateral deformation of the PT span between S1 and S2.

At S1, the gap reduction was found to be 0.8 mm, compared with 0.64 mm at S2. Spacer wear and local deformation of the CT (gap reduction in the industry reports) may be contributing factors but the mechanisms of gap reduction at the spacers are not considered here.

For the time-to-contact analysis with the as-measured gap profile, 0.64 mm, for S2 was used as the amount of spacer gap reduction over a period of 161,000 EFPH. For the analysis with the calibrated gap profile, a spacer gap reduction of 0.32 mm was used, which is less conservative and results directly from gap calibration. It should be noted that the time-to-contact results are not influenced by the choice of 0.8 mm or 0.64 mm as the spacer gap reduction value.

The lateral deformation of the PT span, depicted in Figure 8, has four components:

1. Creep sag of the PT due to in-service lateral loading under irradiation
2. A very small amount of elastic deformation due to the weight of the PT
3. A slight amount of elastic deformation due to the weight of the coolant in the PT during the inspection
4. A slight amount of elastic deformation due to the weight of the inspection tool inside the PT during the inspection.

At this point, it must be noted that the time-to-contact predictions are based on the in-service gap profile, which is different to the as-measured and the calibrated gap profiles.

Therefore, a significant step in calculating the time of CT to PT contact is the conversion of the as-measured or calibrated gap profiles to the in-service gap profile, as detailed below

For the as-measured gap profile of Figure 8, which, to reiterate, has no gap calibration, and for the calibrated gap profile of Figure 9, time-to-contact predictions were generated along the following steps:

1. Uniformly Distributed Loads (UDLs) were obtained for (a) the weight of the PT, (b) the weight of the coolant in the PT during inspection, (c) the weight of the fuelled PT and the concentrated load due to the weight of the inspection tool was obtained. Note that (a)+(b)+(c) represents the total vertical loading on the PT during inspection.
2. Elastic lateral deflections were calculated for the potential contact point in the PT span of Figure 8 under the UDLs of cases (a), (b), and (c) and under the concentrated load of the inspection tool.
3. The gap profile of Figure 8 was adjusted to remove elastic deformations of the PT span resulting from lateral loading during the inspection (UDL (a), UDL (b), and the load of the inspection tool). The adjusted profile gave the gap reduction at the potential contact point due to creep sag of the PT combined with gap reduction at the spacer, necessary to calculate time-to-contact.
4. The rate of creep sag for the potential contact point on the PT was determined.
5. The rate of gap reduction at the spacers was determined.
6. From Steps 4 and 5, the gap closure rate for the potential contact point on the PT, assumed to be constant with time, was found as the sum of the spacer gap reduction rate and the creep sag rate for the potential contact point on the CT.
7. The as-measured gap profile was adjusted to account for UDL (a) and UDL (c) on the PT, representing the normal operating lateral load on the PT. This gave the actual in-service gap at the potential contact point on the PT at 161,000 EFPH.
8. Knowing the gap at 161,000 EFPH from Step 7, and the gap closure rate from Step 6, the time-to-contact was predicted.

A summary of the time-to-contact calculations is presented below.

### 3.3.4.1 Summary of UDL Calculations

The UDL and weight values used to determine the changes in the gap at potential contact point on the PT, due to elastic deflection, are presented below in Table 2.

**Table 2**  
**UDL Values and Inspection Tool Weight for the PT Span of Figure 8.**

UDL Values							Weight
Fuel	PT	D <sub>2</sub> O Fuelled	Fuel + D <sub>2</sub> O	Fuelled PT	D <sub>2</sub> O Alone	Inspection	Wt <sub>Tool</sub>
(N/m)	(N/m)	(N/m)	(N/m)	(N/m)	(N/m)	(N/m)	(mN)
475.316	92.202	34.52	509.840	602.042	95.236	187.438	0.00020

Note that fuel denotes the lateral UDL of the fuel bundles loading the PT. The inspection UDL consists of the distributed load from the weight of the coolant in the PT during inspection plus the distributed weight of the PT.  $Wt_{Tool}$  is the estimated weight of the inspection tool.

The fuelled PT UDL of 602 N/m is the weight/length of the fuel plus coolant in the PT plus the PT and is the UDL on the PT during normal operation of the reactor.

D<sub>2</sub>O stands for the primary heat transport coolant.

### 3.3.4.2 Summary of Elastic Deflection Calculations for the Potential Contact Point on the PT

For the elastic deflection calculations, the PT span of Figure 8 was treated as a straight, elastic beam, simply supported at each end. For the case of uniform loading, as in Tables 3 and 4, the mid-span deflection was based on Table X from Reference [4]. For point loading, as in Table 5, the mid-span deflection was based on Table X from Reference [4]. The PT span was assumed to have design basis inner and outer diameter values.

Tables 3 and 4 provide summaries for the elastic deflection calculations under different UDLs. Table 3a defines the symbols used in Tables 3, 4, and 5. Table 3 is for the UDL on the PT span during inspection, noting that the loading condition does not include the weight of the inspection tool. The elastic deflection from the weight of the inspection tool is treated separately in Table 5.

Table 4 is similar to Table 3 but features the UDL acting on the PT for normal operation of the reactor.

**Table 3**  
**Elastic Deflection of the Potential Contact Point on the PT Under the UDL During Inspection**

A	$w_a$ (N/m)	$l$ (m)	E (Pa)	$R_{OPT}$ (m)	$R_{IPT}$ (m)	I (m <sup>4</sup> )	y (m)	y (mm)
1	187.438	1.041	1.04E+11	0.0566	0.05241	2.135E-06	-2.58E-06	-2.58E-03

**Table 3a**  
**Definition of Symbols for Tables 3, 4, and 5**

A	Constant for End Conditions
$w_a$	Load per Unit Length
$l$	Span Length
E	PT elastic Modulus
$R_{OPT}$	PT Outer Radius
$R_{IPT}$	PT inner Radius
I	PT Cross-Section Area Moment of Inertia
y	Elastic Deflection

**Table 4**  
**Elastic Deflection of the Potential Contact Point**  
**on the PT Under the Fuelled UDL**

A	$w_a$	$l$	E	$R_{OPT}$	$R_{iPT}$	$I$	$y$	$y$
	(N/m)	(m)	(Pa)	(m)	(m)	(m <sup>4</sup> )	(m)	(mm)
1	602.042	1.041	1.04E+11	0.0566	0.05241	2.135E-06	-8.29E-06	-8.29E-03

In Table 5,  $Wt_{Tool}$  is the estimated weight of the inspection tool that was inserted into the PT to measure the CT-PT gap. As before, the PT span of Figure 8 was modelled as a straight elastic beam. For the deflection calculation, it was assumed that gap measured at the potential contact point was recorded when the inspection tool was at the mid-span location.

**Table 5**  
**Elastic Deflection of the Potential Contact Point**  
**on the PT Under the Weight of the Inspection Tool**

A	$Wt_{Tool}$	$l$	E	$R_{OPT}$	$R_{iPT}$	$I$	$y$	$y$
	(N)	(m)	(Pa)	(m)	(m)	(m <sup>4</sup> )	(m)	(mm)
1	200	1.041	1.04E+11	0.0566	0.05241	2.135E-06	-2.76E-06	-2.76E-03

### 3.3.4.3 Summary of the Comparative Time-to-Contact Predictions for the Potential Contact Point on the PT

A summary of the comparative time-to-contact predictions is presented in Table 6. Case 1 in Table 6 is for the as-measured gap profile of Figure 8 and Case 2 is for the calibrated gap profile of Figure 9.

Table 6 provides the predicted fuelled gap at  $x$ , which is the axial location of the potential contact point, and the gap closure rate, which is the sum of the gap reduction rate at the spacer and the creep sag rate at  $x$  on the PT, also given in Table 6. Note that the creep sag rate for the potential contact point on the PT span of Figure 8 amounts to the rate of gap reduction at the point in question. Knowing the fuelled gap at  $x$  at 161,000 EFPH, (which is for normal operating conditions) and the gap closure rate, (assumed to be constant) the time-to-contact was calculated directly both with and without gap calibration. The time-to-contact predictions appear in the last column of Table 6.

**Table 6**  
**Summary of the Comparative Time to Contact Predictions with and without**  
**Gap Calibration for the Potential Contact Point on the PT**

Case	$x$	Gap	Gap at $x$ from Creep Sag	Creep Sag at $x$	EFPH	Creep Sag Rate	Fuelled Gap at $x$	Spacer Gap Reduction	Spacer Gap Reduction Rate	Gap Closure Rate at $x$	Time-to-contact at $x$
	(mm)	(mm)	(mm)	(mm)	(kh)	(mm/EFPH)	(mm)	(mm)	(mm/EFPH)	(mm)	(EFPH)
1	1870.4	3.430	3.436	1.509	161	9.375E-06	3.427	0.64	4.006E-06	1.338E-05	417125
2	1897.9	4.140	4.145	1.124	161	6.979E-06	4.137	0.32	1.994E-06	8.973E-06	622061

From Table 6, the measured and calibrated gaps are practically unaltered by the removal of the UDL during inspection and the weight of the inspection tool. It can be seen that gap calibration significantly increases the gap at the potential contact point at 161,000 EFPH but also assumes a lower rate of gap reduction at the spacer locations. These two combined effects result in a significantly greater time-to-contact prediction for the case of gap calibration versus that for the use of the as-measured (uncalibrated) gap profile.

In this particular example, the increase in time-to-contact from the use of gap calibration is immaterial to the integrity of the Fuel Channel, since both 417 and 622 kEFPH are well above the original Fuel Channel design life of 210 kEFPH. However, in this case gap calibration results in a 49% increase in time-to-contact compared to the time-to-contact using the as-measured gap profile.

Although it is possible that the time-to-contact predictions for the PNGS Fuel Channels could also be acceptable without gap calibration, gap calibration is less conservative than the use of as-measured gaps and may not be technically justifiable because of the implications of gap calibration for CT ID profiles, described in this report.

#### 4. Review of Reference [2]

A technical review of the text in Reference [2] related to Fuel Channel fitness-for-service was conducted, as stated previously. The review was focused primarily on Appendix I of Reference [2]. Column 3 of Table 7, presented below, quotes the sections of the text that were commented on. The corresponding comments were recorded in Column 4 of Table 7.

**Table 7  
Summary of the Review of Reference [2]**

<b>Comment No.</b>	<b>Page No.</b>	<b>Text</b>	<b>Comment</b>
1	181	Pressure tube failure is a design-basis event for CANDU reactors, which have built-in mitigating capabilities that would ensure that the releases into the environment would be small and dose to the public would be within the prescribed dose limits should this event occur.	The text gives the impression that PT failure is a relatively frequent event, largely because of the reference to a design basis event. It should be emphasized that a PT rupture would likely result in no release (not a small release) to the public.
2	187	Table I1, Row 1 Update finite element software to simulate outlet rolled joint Heq evolution....	In reality, it is expected that this task will prove to be minor. The update should not require coding but just a change to the input file to specify a circumferential temperature gradient. The point here is that existing software does not need a fundamental rewrite, just a more sophisticated input file that reflects the recently implemented circumferential

			temperature gradient at the outlet rolled joint.
3	187	Table I1, Row 2 Develop finite element software to simulate inlet rolled joint Heq evolution	In reality, it is expected that this task will prove to be minor. The update should not require coding but just a change to the input file to specify a circumferential temperature gradient. The point here is that existing software does not need a fundamental rewrite, just a more sophisticated input file that reflects the recently implemented circumferential temperature gradient at the outlet rolled joint.
4	187	Table I1, Row 4 Improve characterization of 'blip' and expected evolution of the inlet region....	The author considers the formation of the blip to be a controversial issue. The explanation by Bruce Power that the PT contacts the inboard region of the endfitting taper appears to be counterintuitive. The plan to characterize the blip further is commendable from an engineering perspective.
5	187	Table I1, Row 7 Enhance modeling of temperature distributions near the outlet rolled joint region of pressure tubes....	In the author's diffusion analysis for the September 20 <sup>th</sup> 2023 intervention, it was determined that existing ASSERT computations for the temperature distribution in deformed CANDU 6 PTs were adequate to predict the observed circumferential deuterium concentration gradients in B6S13. However, it was noted that detailed PT-specific operating temperatures should be developed for future PT-specific diffusion analyses and this recommendation has been accepted by Bruce Power.
6	187	Table I1, Row 8 Define input parameters required for interim updates to the Heq model	It is proposed that the input parameters should be (1) initial hydrogen (2), diffusion coefficient, temperature distribution, (3) applied hydrostatic stress distribution (depending on forces and moments applied to the PT), (4) the molar volume of hydrogen or deuterium in the PT material.

7	187	Table I1, Row 9 Develop interim Heq model	It may be possible that a final model could be generated directly. However, the strategy of first developing an interim model will prove to be beneficial from the perspective of quality assurance.
8	188	Table I1, Row 14 Complete hydride related crack initiation experiments for unirradiated material at Heq of 220 ppm or higher.	The practical usefulness of the experiments on unirradiated material is debatable since any PT material at 220 ppm or higher would have irradiated material properties. However, from a quality assurance perspective, experiments on unirradiated material are commendable in that they will provide (1) independent test results that can be used to judge the validity of tests on irradiated material, (2) test data that demonstrates the effect of irradiation on crack initiation.
9	189	Table I1, Row 15 Complete fatigue crack initiation experiments for unirradiated material at Heq of 220 ppm or higher	The practical usefulness of the experiments on unirradiated material is debatable since any PT material at 220 ppm or higher would have irradiated material properties. However, from a quality assurance perspective, experiments on unirradiated material are commendable in that they will provide (1) independent test results that can be used to judge the validity of tests on irradiated material, (2) test data that demonstrates the effect of irradiation on fatigue crack initiation.
10	189	Table I1, Row 16 Complete crack initiation experiments for irradiated material with elevated Heq without flaws present	Despite pre-irradiation, the irradiated crack initiation specimen will be subjected to significantly different conditions during the in-laboratory testing, compared with the actual PT material under operating conditions. The conditions include (1) exact temperature distributions, (2) applied stress distribution, (3) Heq distribution and diffusion, (4) the effects of neutron irradiation, (5) the potential effects of in-service



			temperature cycles. The industry's position is that the in-laboratory tests are conservative simulations of crack initiation in the material of in-service PTs. There are indications that the laboratory crack initiation tests are highly conservative. This should be investigated or at least documented by the industry.
11	189	Based on the review of the R&D plans and the first update, CNSC staff conclude that Bruce Power and OPG continue to target the key issues raised regarding pressure tube fitness for service with respect to the elevated Heq discoveries.	Under the topic of elevated Heq, the CANDU operators are fortunate that hydrogen/deuterium has been seen to be diffusing from the bottom of the PT (where flaws can be present) to the top of the PT where no mechanism for flaw generation has been found. It is recommended that the industry should make use of this fact in fitness-for-service assessments and be acknowledged by the CNSC.

## 5. Conclusions

1. In the review of References [1] and [2], no significant issues related to Fuel Channel fitness-for-service were discovered.
2. However, further investigations by the author (to be verified in the intervention) have indicated that calibration of measured CT-PT gap profiles has been ongoing in the industry and that gap calibration has been used in the assessment of the PNGS Fuel Channels.
3. Based on gauging results from ex-service CTs, in-service CTs are expected to have a nearly uniform mean CT ID profile over the length of the CT. In contrast, the mean CT ID profiles produced using inspection data with gap calibration are notably non-uniform over the length of the CT while those produced using as-measured gap values are uniform. This finding indicates that gap calibration may be technically unsound and further work will be required to justify gap calibration.
4. The use of calibrated gaps versus as-measured (uncalibrated) gaps results in the prediction of greater times-to-contact. Therefore, gap calibration produces less conservative time-to-contact results than those from the use of as-measured gaps. Should gap calibration be shown to be invalid, then the PNGS time-to-contact predictions that use gap calibration would be non-conservative and should be reassessed.

## 6. References

1. Mid-Term Update of Licensed Activities for the Pickering Nuclear Generating Station, CMD 23 M36.1, Written Submission from Ontario Power Generation, 2023-08-31, File 6.02.04.
2. Regulatory Oversight Report for Canadian Nuclear Power Generating Sites for 2022, CMD 23-M36, CNSC Staff, 31 August 2023.
3. *The Generation of Calandria Tube (CT) Inner Diameter Profiles from Fuel Channel (FC) Inspection Data*, 35<sup>th</sup> Annual Conference of the Canadian Nuclear Society, Saint John, NB, May, 2015.